

PHOTOPHYSICAL PROCESSES IN COUMARIN SENSITIZERS

O. N. Tchaikovskaya, E. N. Bocharnikova,
N. G. Dmitrieva, and I. V. Sokolova

UDC 539.194:535.37

The quantum-chemical and spectroscopic methods make it possible to record the features of photoactivated processes occurring within and between molecules, as well as the structural rearrangements of molecules. To solve the fundamental problem of establishing a relationship between the photophysical and spectral-luminescent properties of organic molecules and their structure, a comparative analysis of the nature of electronically excited states and photoprocesses in coumarin and its related compounds (furocoumarin and 8-methoxypsoralen) has been carried out. To understand the mechanism of forming the absorption and fluorescence spectra of compounds, the schemes of electronically excited states of the molecules under study and the charge localization on the molecular orbitals have been calculated and analyzed. The investigated compounds are effective sensitizers, and the presence of the OCH₃ group in the molecular structure has the strongest effect on the spectral-luminescent characteristics. This paper presents the results of studying the induced absorption spectra of 8-methoxypsoralen by the pump-probe method with a delay of 30 ns in the range of 350–700 nm. The experimentally recorded induced absorption of 8-methoxypsoralen belongs to long-living photoproducts of a radical nature.

Keywords: coumarin, psoralen, absorption, fluorescence, photophysical processes, quantum chemical calculation, 8-methoxypsoralen.

INTRODUCTION

Coumarin, also called *coumarou*, is a representative of the group of polyphenolic compounds first extracted from tonka beans (*Dipteryx Odoranta* Wild; *Fabaceae* family) by Vogel [1] in 1820. Since then the extraction of coumarin compounds from plants, bacteria, and mushrooms [2–4] is repeatedly reported together with the structural characteristic and biological activity of thousands of natural coumarins and their chemical synthesis [5–7]. Coumarins are secondary metabolites of plants whose biological activity varies depending on the character of their substitution. The attention of the modern scientific community is focused on a study of photophysical properties of this compound and its derivatives, because the compounds of this class with various photophysical and photochemical properties are used in optics, green chemistry, radiation chemistry, photobiology, medicine, quantum electronics, and other branches of science and technology [8–10].

For example, many coumarins possess intensive fluorescence used to develop fluorescent labels, sensors, optical brighteners, and laser-active media [11]. Coumarins possessing weak fluorescence are used for water purification or as antioxidants [12]. Furocoumarins (or psoralens) are used in medicine for photochemotherapy of some diseases (psoriasis, vitiligo, mycosis, etc.). The most carefully studied is PUVA therapy used for treatment of dermatoses [13–17]; it allows the frequency of treatment procedures to be reduced to weekly procedures and then to less than one procedure per month maintaining the treatment efficiency and well tolerated irradiation dose [18]. The 8-methoxypsoralen (8-MOP) compound having high photosensitizing activity does not influence directly on the skin

National Research Tomsk State University, Tomsk, Russia, e-mail: tchon@phys.tsu.ru; bocharnikova.2010@mail.ru; brjantseva@rambler.ru; sokolova@phys.tsu.ru. Translated from *Izvestiya Vysshikh Uchebnykh Zavedenii, Fizika*, No. 8, pp. 40–48, August, 2020. Original article submitted July 6, 2020.

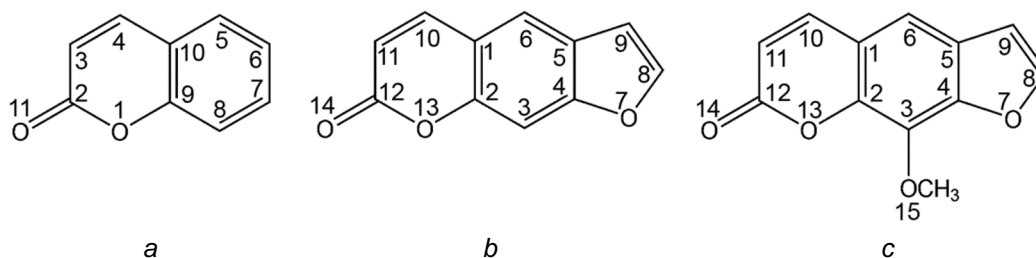


Fig. 1. Structural formulas of the investigated molecules: *a* – unsubstituted coumarin, *b* – psoralen, and *c* – 8-methoxypsoralen.

affected by psoriasis, and becomes active only after exposure of the organism to UV radiation. It enters into the reaction with epidermal cells and suppresses excessive DNA replication without suppression of cellular functions [13]. However, the high photosensitizing activity of 8-MOP can complicate its administration to patients with gentle skin and vitiligo because of the risk of patient burn. At present, the administration of photosensitizers in medicine requires that they have the following characteristics: a) preferential localization in affected organs, b) fast clearance from healthy tissue, c) effective absorption in the so-called *therapeutic window* (600–1000 nm) with low light scattering in tissues, and d) no toxicity or low toxicity of the preparation.

The search for new photosensitizers with improved properties requires knowledge of their photophysical and photochemical characteristics. The rate constants of the photophysical processes in molecules after absorption of quantum of light determine the subsequent photochemical reactions with participation of electronically excited states, mostly triplet, and hence, the photobiological processes. The establishment of fundamental regularities of changes in the properties of molecules depending on their structure will allow the purposeful search to be carried out and the risk of complications during treatment of various diseases to be reduced. This work studies processes of the electronic excitation energy deactivation in furocoumarin 8-MOP molecules by the methods of electronic spectroscopy and quantum chemistry.

OBJECTS AND METHODS OF RESEARCH

Unsubstituted coumarin, psoralen (furocoumarin), and 8-methoxypsoralen (8-MOP) were chosen as objects of research. The structural formulas of the compounds are shown in Fig. 1. In this work, we used 8-MOP produced by Aldrich. Bidistilled water and ethanol (Merck) were used as solvents. The 8-MOP characteristics were interpreted by means of their comparison with the data obtained for psoralen and coumarin molecules. The investigated compounds are well soluble in organic solvents and poorly soluble in water. They are easily soluble in water solutions of alkalis with opening of the lactone ring and forming salts of hydroxycinnamic acid [19, 20]. The spectral-luminescent characteristics of solutions were registered using an SM2203 spectrofluorimeter (SOLAR, Belarus) [21], an Evolution-600 spectrofluorimeter (Thermo Scientific), and a Cary Eclipse spectrofluorimeter (Varian) equipped with an Optistat DN cryostat. A XeCl excilamp with radiation wavelength $\lambda_{\text{rad}} = 308$ nm was used as a source of UV radiation.

Theoretical studies were performed using the software package based on the semiempirical *INDO/S* method. To solve spectroscopy problems, we used quantum chemical programs and procedures for estimation of the rate constants of photoprocesses developed by Professor G. V. Mayer, Professor V. Ya. Artyukhov, Assistant Professor A. I. Galeeva, and Assistant Professor V. A. Pomogaev [22–25]. The software package permits determination of the following characteristics of the electronic states of polyatomic molecules: the energy and the nature of the molecular orbitals, the energy and the wave functions of the singlet and triplet electronically excited states, the oscillator strengths, the polarization of the electronic transitions, the distribution of the electronic density over atoms and molecular bonds, the dipole moments of the ground and excited states, and the absorption and fluorescence spectra. The geometry was optimized by the *AM1* and *PM3* quantum chemical methods [26]: *AM1* is Austin Model 1 and *PM3* is Parametrical Model 3. In comparison with the *MNDO* method, the *AM1* method eliminated the overestimation of the long-range

interaction between the atoms leading to the overestimation of the barriers of internal rotation in molecules. As a result, correct calculation of the hydrogen bonds became possible that in the *MNDO* method were possible only for special modifications. The *PM3* method used a refined set of the parameters of the *AM1* method and as a whole, had the same advantages and disadvantages. The methods considered in the present work permit calculations of a large number of the molecular characteristics [27–29].

To study the induced absorption spectra, the experimental setup intended for registration of the spectra of nonstationary differential absorption by the pump-probe method with a fluorescent probe was used. The setup provided nanosecond time resolution. Its optical scheme, operating principle, and procedure of signal processing were described in [30]. The setup allowed the absorption spectra of the short-living states and products, for example, of singlet-singlet ($S_1 \rightarrow S_n$) absorption, and of the long-living states (with lifetimes exceeding the pump pulse duration), for example, of the triplet-triplet ($T_1 \rightarrow T_m$) absorption of molecules to be identified. The third harmonic (355 nm) of a pulsed Nd:YAG laser with Q-factor modulation, $\tau_{1/2} = 7$ ns, and $E_{\text{pulse}} = 20\text{--}40$ mJ was used for pumping. As a probing radiation, the fluorescence of a mixture of dye solutions (in the region of 350–750 nm with luminescence pulse duration of 9 ns), excited by the same pump laser, was used. The delay line was 10 m long, thereby providing a delay time of about 30 ns.

RESULTS AND DISCUSSION

To analyze the spectral-luminescent properties of the coumarin dyes, the properties of its frame structure – the unsubstituted coumarin molecule (Fig. 1a) – should primarily be studied. For this molecule, many articles have been published in the literature, in which the energy level diagrams, defining the specific structure of the coumarin molecule, are presented. Unsubstituted coumarin at room temperature does not fluoresce or phosphoresce. J. B. Gallivan [31] performed the careful analysis of the spectral properties of the unsubstituted coumarin molecule. He showed that the temperature decrease activated the coumarin luminescence in polar and nonpolar solvents, and radiation was different in character depending on the polarity of the solvent. In the nonpolar solvents at 77 F, the fluorescence dominated (at $\lambda_{\text{fl}} = 390$ nm, the ratio of the phosphorescence to fluorescence quantum yields was $\varphi_{\text{ph/fl}} = 0.02$). In the polar solvents at low temperatures, the intense phosphorescence (with a lifetime of 0.45 s) and the weaker fluorescence ($\varphi_{\text{ph/fl}} = 5$) at longer wavelengths compared to the nonpolar solutions ($\lambda_{\text{max}} = 417$ nm) were observed without vibrational structure. J. B. Gallivan explained such unusual behavior of the unsubstituted coumarin radiation by the formation of fluorescing aggregates (excimers) in the nonpolar solvents and by radiation from the Franck–Condon states in the polar solvents. However, in [32] it was shown that fluorescing excimers were formed only in the presence of benzophenone sensitizer, and that the fluorescing dimers were formed only in water solutions with high unsubstituted coumarin concentrations. Therefore, it was reasonable to search for a solution in the photophysics of the unsubstituted coumarin molecule.

The analysis of the absorption spectra of unsubstituted coumarin in [31] showed that there was no noticeable change in the position of the absorption band at $\lambda_{\text{max}} = 312$ nm when the solvent changed. Experimental data suggested that the longest-wavelength absorption band at $\lambda_{\text{max}} = 323$ nm has the $n\pi^*$ type. Moreover, the high values of the molar absorption coefficient (ϵ) and the oscillator strength (f) suggested that very close $\pi\pi^*$ and $n\pi^*$ electronic states were mixed. The presence of the kink in the long-wavelength band was also observed by J. B. Gallivan, but he did not interpret this fact at all. One more experimental evidence of the presence of the $n\pi^*$ -type absorption band at 320 nm was a little change in the direction of the dichroism curve around this wavelength. However, T. Minegishi *et al.* [32], just like J. B. Gallivan, ignored this fact and considered that the first absorption band was the $\pi\pi^*$ band ($\lambda = 310$ nm), which gave him grounds to carry out quantum chemical calculations in the π -electronic approximation.

Based on the obtained data on the position of the singlet and triplet states, the energy level diagram for the investigated compounds is plotted in Fig. 2. The lower singlet level of unsubstituted coumarin is the $n\pi^*$ level, and two $\pi\pi^*$ levels of different natures are located higher on the energy axis. The $S_0 \rightarrow S_1$ ($n\pi^*$) singlet transition is polarized perpendicularly to the plane of the molecule and is associated with the transition of n electrons of the carbonyl oxygen atom to the π orbitals of the carbon atoms mainly in positions 4, 3, and 7. Two lower singlet $\pi\pi^*$ transitions ($S_0 \rightarrow S_2(\pi\pi^*)$ and $S_0 \rightarrow S_3(\pi\pi^*)$) are polarized along the long axis of the molecule, but in the opposite directions, that is in agreement with the experimental data presented in [31].

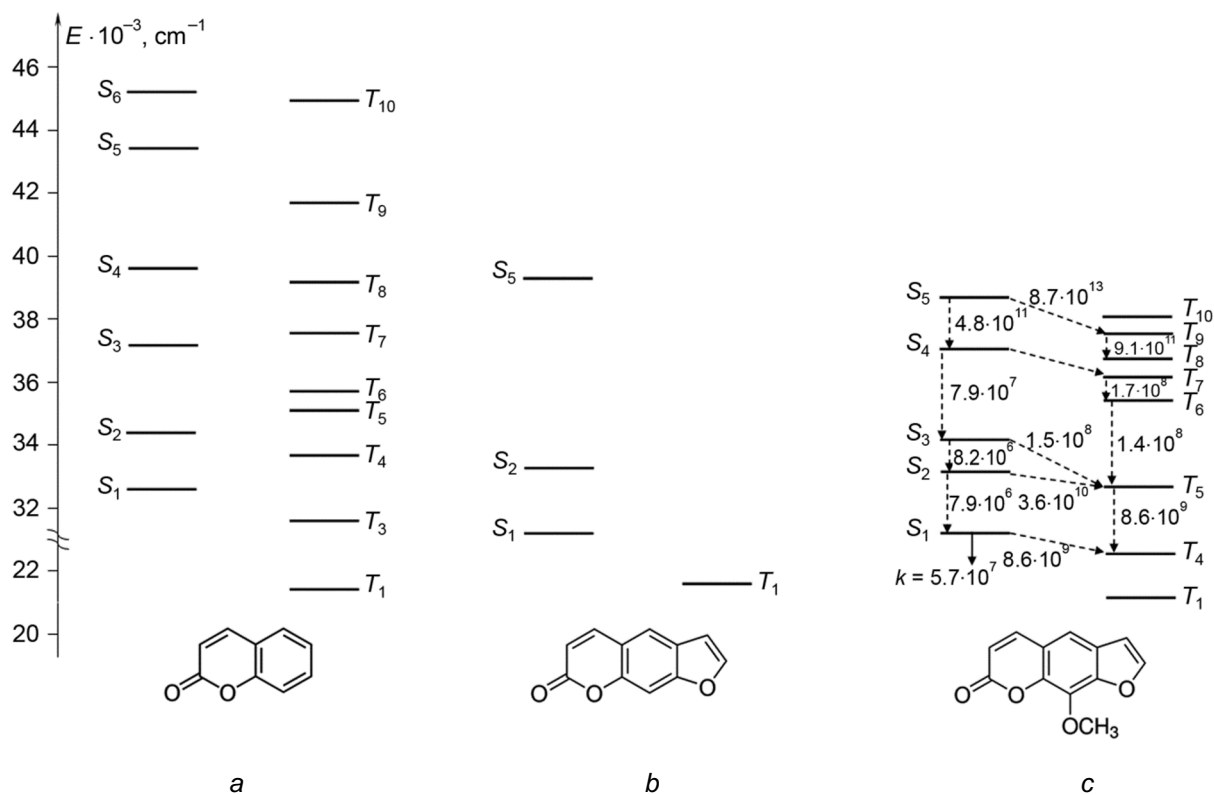


Fig. 2. Energy level diagrams of the electronically excited states of isolated molecules: *a* – unsubstituted coumarin, *b* – furocoumarin (psoralen) [31], and *c* – 8-methoxypsoralen (8-MOP).

The analysis of the calculated data showed that the first resolved singlet $\pi\pi^*$ transition ($S_0 \rightarrow S_2$) is associated largely with the redistribution of the electronic density between carbons of both rings rather than with the absorption of the pyrone moiety according to the assumption of S. C. Haydon [33], namely, the carbon atom in position 7 (Fig. 1) is substantially involved in the charge transfer, and the electronic density is transferred from the benzene ring to the carbon atom in position 7, thereby considerably increasing the negative charge and the population of the π orbital.

When the $\pi\pi^*$ transition ($S_0 \rightarrow S_3$) of the unsubstituted coumarin is formed, the electronic density from the oxygen atoms and almost all carbon atoms of the pyrone ring (except C_4) goes on the aromatic ring and the carbon atom in position 4 (Fig. 1). The carbon atom in position 7 makes the greatest contribution to the formation of the transition moment. A special role of the carbon atom in position 7 in the formation of the $S_0 \rightarrow S_3$ transition should also be noted. When the energy is absorbed, a significant part of the electronic density is transferred to the aromatic ring of the unsubstituted coumarin molecule, and the electronic charge of the π orbital is depleted, in other words, the decrease of the negative charge on this atom is observed. Therefore, the spectral properties of unsubstituted coumarin are caused mainly by the redistribution of the electronic density among the carbon atoms in positions 3, 4, and 7. The substitution exactly in these positions leads to the most effective fluorescence of the compounds. Moreover, S. M. Souza *et al.* [34] experimentally studied 45 different compounds of substituted coumarin and established that the incorporation of the OH group in position 7 is important for the antibacterial activity of the molecule against the *Bacillus cereus* MIP 96016, *Escherichia coli* ATCC 25922, *Pseudomonas aeruginosa* ATCC 27853, and *Staphylococcus aureus* ATCC 25923 strains. The good agreement between the experimental and calculated $S_0 \rightarrow S_7$ (217 nm) and $S_0 \rightarrow S_{10}$ (200 nm) absorption bands of unsubstituted coumarin should also be noted, which gives us grounds to rely on the data of quantum chemical calculation of highly excited states of coumarin derivatives for which experiments are lacking.

The quantum chemical calculation demonstrated that 8-MOP (Fig. 2c) has several electronic transitions in the spectral range up to 240 nm. It should be noted that the inversion of the singlet excited states of the $\pi\pi^*$ and $n\pi^*$ types

TABLE 1. Oscillator Strengths (f) and Energies of 8-MOP Used in the Employed *AM1* and *PM3* Calculation Methods

State	E_i, cm^{-1}		f	
	<i>AM1</i>	<i>PM3</i>	<i>AM1</i>	<i>PM3</i>
$S_1(\pi\pi^*)$	31673	32239	0.080	0.109
$S_2(n\pi^*)$	33637	33845	0.0001	0.0001
$S_3(\pi\pi^*)$	34066	35070	0.188	0.143
$T_1(\pi\pi^*)$	15731	16116	0.150	0.146
$T_2(\pi\pi^*)$	21222	21379	0.645	0.664
$T_3(\pi\pi^*)$	23280	23750	0.031	0.041
$T_4(\pi\pi^*)$	26207	27047	0.269	0.308
$T_5(\pi\sigma^*)$	30312	31187	0.521	0.462

takes place in 8-MOP compared to the coumarin and psoralen molecules [35]. Table 1 presents the energy values and the oscillator strengths of 8-MOP. The first singlet excited level is of the $\pi\pi^*$ type.

The quantum fluorescence yields of molecules in ethanol were estimated from their fluorescence spectra by the relative method. The experimental and calculated data demonstrate that 8-MOP possesses a weak fluorescent ability. For the investigated compounds, the experimental values of the quantum fluorescence yields are in good agreement with the data for the compounds with related structure (0.01–0.025 for psoralen and 0.0013 [35, 36] for 8-MOP at $T = 298 \text{ K}$). Because 8-MOP poorly fluoresces, of interest is the research of the main excitation energy deactivation channels. The 8-MOP compound has one excitation energy deactivation channel through the system of triplet states: $S_3 \rightarrow T_8 \rightarrow \dots \rightarrow T_1$. It was established that for all investigated molecules, the effective intersystem crossing takes place with rate constants of $\sim 10^{13} - 10^{10} \text{ s}^{-1}$ because of the close arrangement of the levels having orbital natures of the $\pi\pi^*$ and $n\pi^*$ types, which leads to low values of the quantum fluorescence yield and considerable population of the T_1 state. The incorporation of the furan rings into the structure of the coumarin molecule leads to the increased efficiency of the intersystem crossing in the investigated compounds.

The long-living triplet states play an important role in many photochemical processes. An analysis of the fluorescence and phosphorescence spectra at a temperature of 77 K demonstrated that the investigated compounds are poorly fluorescing at room temperature. The 8-MOP fluorescence spectrum is located at shorter wavelengths compared to furocoumarin and unsubstituted coumarin. The most weakly fluorescing at temperatures of 77 and 298 K was 8-MOP. The results of experimental investigation of the fluorescent properties of 8-MOP at room temperature were in agreement with the data presented in [36, 37]. With decreasing temperature, the maxima of the bands in the fluorescence spectra of all compounds shifted toward shorter wavelengths, and the quantum fluorescence yields increased. This is due to the fact that the molecule becomes more rigid, and the probabilities of nonradiative processes decrease. The phosphorescence spectrum of 8-MOP is located at longer wavelengths compared to the phosphorescence spectra of coumarin and furocoumarin. The data on the position of the bands (λ_{fl} and λ_{ph}) and the quantum fluorescence (φ_{fl}) and phosphorescence yields (φ_{ph}) of 8-MOP in the water-ethanol solution obtained in the work are in agreement with the data presented in [38]: $\lambda_{fl} = 470 \text{ nm}$ at $T = 298 \text{ K}$; $\lambda_{fl} = 440 \text{ nm}$ and $\varphi_{ph} = 0.0013$ at $T = 77 \text{ K}$; $\lambda_{ph} = 457 \text{ nm}$ and $\varphi_{ph} = 0.17$.

The photochemical reactions proceed with participation of the triplet states of photosensitizer and oxygen molecules. Therefore, the effect of oxygen presented in solutions on the photophysical properties of substituted coumarin was investigated. To estimate the effect of oxygen on the luminescent properties of the investigated series of compounds, the quantum luminescence yields were determined and the phosphorescence lifetimes both in oxygen-containing and deoxygenated solutions were measured. From Table 2 it follows that the quantum phosphorescence yield of 8-MOP increased. Taking into account the experimentally measured quantum luminescence yields and the phosphorescence lifetimes, the rate constants of the $T_1 \rightarrow S_0$ crossing were estimated. For the investigated series of compounds, these values increased from 0.2 to 1.4 s^{-1} . From the data presented in Table 2 we have concluded that the presence of oxygen has no effect on the phosphorescence lifetime of the frozen solutions of the investigated

TABLE 2. Stokes Shift ($\Delta\nu_{ST}$), Band Maximum (λ), Phosphorescence Lifetime (τ_{ph}), and Quantum Fluorescence Yield (ϕ) of 8-MOP at the Indicated Temperatures

Calculation*	Experiment**							
	Fluorescence				Phosphorescence			
	298 K			77 K		77 K		
ϕ_{th}	λ , nm	$\Delta\nu_{ST}$, cm^{-1}	ϕ	λ , nm	ϕ^{***}	λ , nm	ϕ^{***}	τ_{ph} , s
0.001	470	11000	0.001 0.0013 [34]	449	0.013 (0.012)	460	0.17 (0.19)	0.55 0.76 [35]

Notes. * Calculation was performed for the isolated molecule. ** Concentration of the investigated compounds in ethanol was 10^{-5} M. ***The quantum yield of deoxygenated solutions.

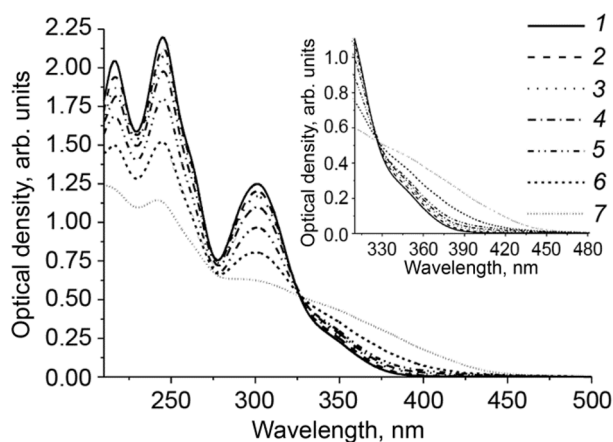


Fig. 3. Absorption spectra of 8-MOP in ethanol for the irradiation time, min: 0 (curve 1), 2 (curve 2), 4 (curve 3), 8 (curve 4), 16 (curve 5), 32 (curve 6), and 64 (curve 7) and 8-MOP concentration of 0.1 mm.

compounds, but it significantly affects the quantum fluorescence and phosphorescence yields. Comparing the phosphorescence lifetime with the structure of the investigated molecules (Fig. 1), we have concluded that the absence of the furan ring in the structure of the coumarin molecule decreases the phosphorescence lifetime compared to the lifetimes of other investigated objects. However, the phosphorescence lifetime obtained by us for 8-MOP (0.55 s) is in agreement with the data presented in [39] for the oxygen-containing solutions of 8-MOP in ethanol (0.65 s).

The absorption maximum of furocoumarin in benzene coincides with the absorption maximum in water. According to [40, 41], the $T-T$ absorption spectrum of furocoumarin is shifted by 10 nm toward the red wavelengths when going from methanol to benzene. Based on the obtained data on the position of the singlet and triplet states and on the rate constants of the photophysical processes in the electronically excited states, the channels of deactivation of the excitation energy were constructed. We can conclude that the investigated compounds are the effective sensitizers, and the presence of the methoxy group in the structure of molecules affects most strongly the spectral-luminescent characteristics of the investigated molecules. Because the photostability is one of the important properties of photosensitizers, we investigated the effect of $XeCl^*$ excilamp radiation ($\lambda_{rad} = 308$ nm, frequency 200 kHz) on the spectral-luminescent properties of substituted coumarins and their photostability in ethanol and water-ethanol solutions (1:1). The dependence of the absorption and fluorescence intensities on the irradiation time was observed (Fig. 3).

With increasing 8-NOP irradiation time, the optical densities for the bands at 246 and 302 nm decreased, and the optical density in the region of 330–420 nm increased. These changes demonstrated the formation of photoproducts. The values of the quantum photodecay yield of 8-MOP upon excitation by $XeCl^*$ excilamp radiation show that the

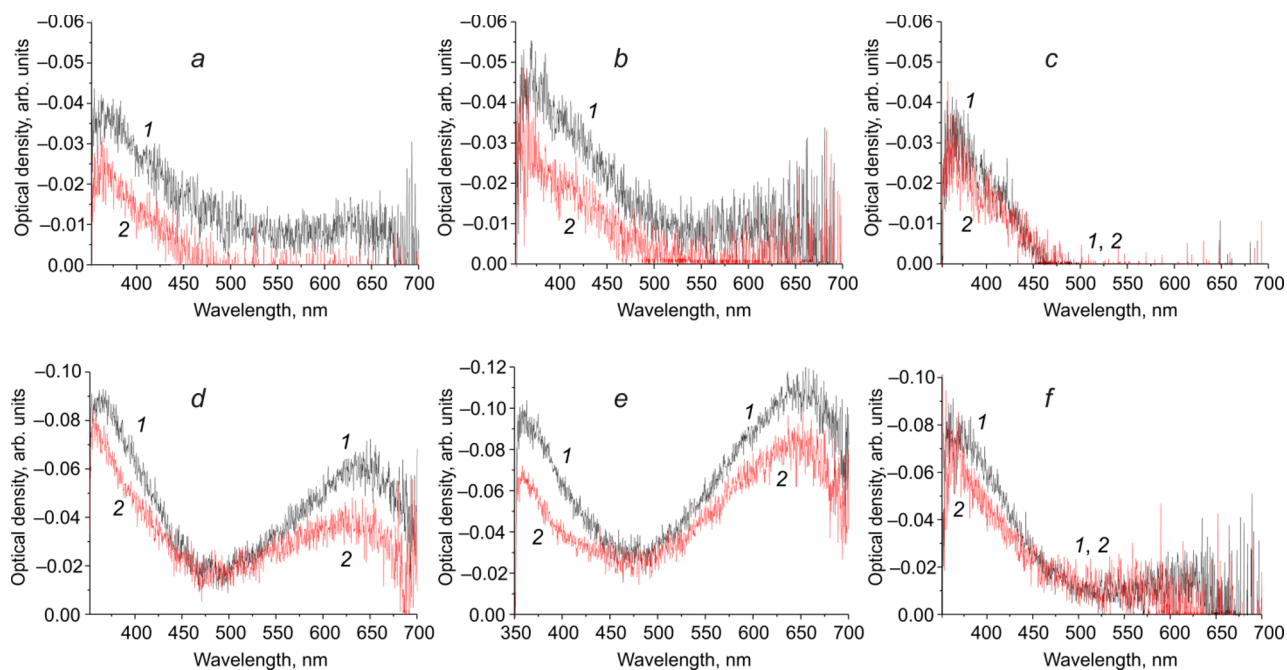


Fig. 4. Induced absorption spectra of 8-MOP with concentration of 0.1 mM in ethanol (a) and with addition of water (d, e, and f) and hydrogen peroxide (b and c) without (curve 1) and with a delay (curve 2) for hydrogen peroxide concentrations of 0.14 mM (b) and 0.28 mM (c), ethanol and water in the ratio 1:1 (d), ethanol and water in the ratios 1:9 (e) and 1:1 (f) with hydrogen peroxide concentration of 0.14 mM.

compound possesses the high photostability. Moreover, the photostability did not change significantly when the ethanol solution was changed by the water-ethanol solution: the quantum photodecay yields were 0.004 and 0.003 for the ethanol and water-ethanol (1:1) solutions, respectively. Apparently, the OCH_3 group in 8-MOP has a shielding effect for the intermolecular interactions and at the same time, changes the reactivity of the molecule because of the increase in the electronic density due to the presence of this group in the reaction centre – the oxygen atoms.

It is obvious that the properties of the triplet states of 8-MOP under conditions close to physiological ones, that is, in water are important for clinical tests and applications. Unfortunately, 8-MOP is practically insoluble in water. Nevertheless, the researchers try to determine the triplet-triplet absorption spectrum of 8-MOP in water. As soon as we pass to water solutions, it becomes necessary to consider the effect of the solvated electron formed upon exposure to a photoexcitation pulse that leads to the formation of ions-radicals [42]. Let us proceed to the interpretation of the induced absorption spectra.

Figure 4 shows the induced absorption spectra observed with a 30 ns delay. The singlet-singlet processes had been finished by this time after the pulse termination. The photoexcitation of the 8-MOP solutions in ethanol during the laser flash caused the formation of the absorption characterized by the presence of the band with maximum λ_{max} in the region of 370–380 nm (curve 1 in Fig. 4a). This band had a shoulder on the long-wavelength side around 410 nm the intensity of which did not change after the delay. R. W. Sloper *et al.* [43] informed on the presence of the band with a maximum around 375 nm in the induced absorption spectra with the lifetime much greater than 10 ps. In addition to this band, the weak band at 650 nm was also observed (Fig. 4a). The yield of this intermediate photoproduct depends on the solvation shell of the 8-MOP molecule. The presence of hydrogen peroxide in the ethanol solution of 8-MOP testified that it is formed from the singlet electronically excited state. After addition of hydrogen peroxide with a concentration of 0.14 mM (Fig. 4b) to the ethanol solution of 8-MOP, the band in the region of 650 nm disappeared with a delay. After addition of hydrogen peroxide with a higher concentration, the band at 650 nm did not appear (Fig. 4c). According to the literature data, the absorption in the region of 370–380 nm corresponds to the photoproduct

which represents an ion-radical of 8-MOP [43, 44]. During photolysis of 8-MOP in water-ethanol solutions with larger amount of water additive, a strong induced absorption was registered at 650 nm (Fig. 4d and e), which changed weakly after a delay (curve 2 in Fig. 4e). The increase in water to 90 % increased the intensity of the absorption band at 650 nm. Addition of hydrogen peroxide resulted practically in the disappearance of the band in this region after a delay (curve 2 in Fig. 4f).

CONCLUSIONS

The substitution in the coumarin molecule leads to the inversion of the system of the singlet electronically excited levels: $S_1(n\pi)$ and $S_2(\pi\pi)$ interchange their positions. This increased the efficiency of the intersystem crossing and the internal crossing in the system of the triplet levels of 8-MOP upon photoexcitation. The experimental and theoretical studies demonstrated that 8-MOP undergoes phototransformation upon exposure to excilamp radiation with a wavelength of 308 nm. 8-MOP has the long-living photoproduct with the lifetime exceeding 30 ns and the photoproduct with the lifetime less than 30 ns. Both these intermediate compounds have the radical nature.

The authors express their gratitude to V. A. Svetlichnyi for the experimental measurement of the induced absorption spectra.

This work was supported in part by the Russian Foundation for Basic Research (Project No. 19-53-51005 NIF_a RFFI-Korea) and Collaborative NRF-RFBR grant (Korean ID: NRF-2019K2A9A1A06100125).

REFERENCES

1. A. Vogel, *Ann. Phys.*, **64**, 161–166 (1820).
2. F. M. Dean, *Fortschr. Chem. Org. Naturst.*, **9**, 225–291 (1952).
3. R. D. H. Murray, J. Mendez, and S. A. Brown, *The Natural Coumarins: Occurrence, Chemistry and Biochemistry*, Wiley, Chichester; New York (1982).
4. R. D. H. Murray, *Chem. Org. Naturst.*, **58**, 1–81 (1991).
5. R. O’Kennedy, R. D. Thornes, *et al.*, *Coumarins: Biology, Applications, and Mode of Action.*, John Wiley & Sons, New York (1997).
6. A. Lacy and R. O’Kennedy, *Curr. Pharm. Des.*, **10**, 3797–3811 (2004).
7. J. Bruneton, *Pharmacognosy, Phytochemistry, Medicinal Plants*, Lavoisier, Paris (1999).
8. K. Rohini and P. S. Srikumar, *J. Thermodyn. Catal.*, **5**, No. 2, 1–3 (2014).
9. A. Stefanachi, F. Leonetti, and L. Pisani, *Molecules*, **23**, No. 2, 250 (2018).
10. M. M. Melough, E. Cho, and O. K. Chun, *Int. J. Publ. Br. Ind. Biol. Res. Assoc.*, **113**, 99–107 (2018).
11. V. G. Plotnikov, V. A. Sazhnikov, and M. V. Alfimov, *High Energy Chem.*, **41**, No. 5, 299–311 (2007).
12. V. V. Nikolaeva, L. G. Antropova, and Myin Pkhyo, *Chem. Chem Technol.*, **28**, No. 6, 104–106 (2014).
13. A. Ya. Potapenko, M. V. Malakhov, and A. A. Kyagova, *Biophysics*, **49**, No. 2, 322–339 (2004).
14. Z. Zarebska, E. Waszkowska, S. Caffieri, and F. Dall’Acqua, *Il Farmaco*, **55**, No. 8, 515–520 (2000).
15. W. L. Morison, *Photodermatol., Photoimmunol., Photomed.*, **20**, No. 6, 315–320 (2004).
16. J. Liano, J. Raber, and L. A. Eriksson, *J. Photochem. Photobiol. A*, **154**, Nos. 2–3, 235–243 (2003).
17. R. S. Becker, S. Chakravorti, C.A. Gartner, and M. de Graca Miguel, *J. Chem Soc. Faraday Trans.*, **89**, No. 7, 1007–1019 (1993).
18. J. Guitart, *JAMA Dermatol.*, **155**, No. 5, 529–531 (2019).
19. Ya. L. Garazd, A. S. Ogorodniichuk, M. M. Garazd, and V. P. Khilya, *Chem. Nat. Compd.*, **38**, No. 5, 424–433 (2002).
20. I. G. Antropova, A. A. Fenin, and A. A. Revina, *Khim. Vys. Energ.*, **41**, No. 1, 1–5 (2007).
21. GOST 12997-84 GSP Products. General Specifications. Technical Conditions BY 100424659.013-2006. Spectrofluorimeter SM 2203.
22. G. Grabner, G. Kohler, G. Marconi, *et al.*, *J. Phys. Chem.*, **94**, 3609–3613 (1990).

23. V. A. Pomogaev, R. R. Ramazanov, K. Ruud, and V. Ya. Artyukhov, *J. Photochem. Photobiol. A*, **354**, 86–100 (2018).
24. V. A. Pomogaev, P. V. Avramov, and K. Ruud, *J. Phys. Chem. C*, **123**, 18215–18221 (2019).
25. V. A. Pomogaev, V. A. Barachevsky, A. R. Tuktarov, *et al.*, *J. Phys. Chem. A*, **122**, 505–515 (2018).
26. G. Kohler and N. Getoff, *J. Chem. Soc. Faraday Trans.*, **72**, No. 10, 2101–2106 (1976).
27. V. Ya. Artyukhov and A. I. Galeeva, *Soviet Phys. J.*, **29**, No. 11, 949–952 (1986).
28. V. A. Blatov, A. P. Shevchenko, and E. V. Peresypkina, *Semiempirical Computational Methods in Quantum Chemistry: A Textbook*, Univer –Group Publishing House, Samara (2005).
29. V. Ya. Artyukhov, T. N. Kopylova, L. G. Samsonova, *et al.*, *Russ. Phys. J.*, **51**, No. 10, 1097–1111 (2008).
30. V. A. Svetlichnyi, *Prib. Tekh. Eksp.*, No. 4, 117–123 (2010).
31. J. B. Gallivan, *Mol. Photochem.*, **3**, No. 2, 191–211 (1970).
32. T. Minegishi, T. Hoshi, and Y. Tanizaki, *J. Chem. Soc. Jpn.*, No. 5, 649–653 (1978).
33. S. C. Haydon, *Spectrosc. Lett.*, **8**, No. 11, 815–892 (1975).
34. S. M. Souza, F. D. Monache, and A. Smania, *Z. Naturforsch. C*, **60**, Nos. 9–10, 693–700 (2005).
35. E. N. Bocharnikova, O. N. Tchaikovskaya, V. Ya. Artyukhov, and N. G. Dmitrieva, *Russ. Phys. J.*, **61**, No. 11, 2033–2041 (2019).
36. K. K. Ho, J. S. Eun, and S. Chil, *Bull. Korean Chem. Soc.*, **12**, No. 5, 554–559 (1991).
37. W.W. Mantulin and P. S. Song, *J. Chem. Soc.*, **95**, No. 16, 5122–5129 (1973).
38. J. S. Seixas de Melo, R. S. Becker, and A. L. Macanita, *J. Phys. Chem.*, **98**, 6054–6058 (1994).
39. T.-I. Lai, B. T. Lim, and E. C. Lim, *J. Am. Chem. Soc.*, **104**, No. 26, 7631–7635 (1982).
40. W. Craw, R. V. Bensasson, J. C. Ronfard-Haret, *et al.*, *Photochem. Photobiol.*, **37**, No. 6, 611–615 (1983).
41. D. Bethea, B. Fullmer, S. Syed, *et al.*, *J. Dermatol. Sci.*, **19**, No. 2, 78–88 (1999).
42. J. A. Parrish, T. B. Fitzpatrick, L. Tanenbaum, and M. A. Pathak, *N. Engl. J. Med.*, **291**, No. 23, 1207–1211 (1974).
43. R. W. Sloper, T. G. Truscott, and E. J. Land, *J. Photochem. Photobiol.*, **29**, No. 5, 1025–1029 (1979).
44. S. Solar and R. Quint, *Int. J. Radiat. Appl. Instrum. C. Radiat. Phys. Chem.*, **39**, No. 2, 171–175 (1992).